AGU PUBLICATIONS

Geophysical Research Letters

RESEARCH LETTER
10.1002/2015GL063191

Key Points:
- Decadal changes in subsurface properties impact the Gulf of Alaska
- Role of subsurface anomalies in upper-ocean temperature
- Subsurface anomalies drive a fraction of the surface decadal variability

Correspondence to:
M. Pozo Buil,
mercedes.pozo@eas.gatech.edu

Citation:
Pozo Buil, M., and E. Di Lorenzo (2015), Decadal changes in Gulf of Alaska upwelling source waters, *Geophys. Res. Lett.*, *42*, 1488–1495, doi:10.1002/2015GL063191.

Received 20 JAN 2015
Accepted 10 FEB 2015
Accepted article online 12 FEB 2015
Published online 13 MAR 2015

Decadal changes in Gulf of Alaska upwelling source waters

Mercedes Pozo Buil[1] and Emanuele Di Lorenzo[1]

[1]School of Earth and Atmospheric Sciences, Georgia Institute of Technology, Atlanta, Georgia, USA

Abstract Decadal changes in sea surface temperature (SST) in the Gulf of Alaska are linked to long-term transitions in the marine ecosystem. While previous studies have identified the atmospheric variability of the Aleutian Low as an important driver of Ekman pumping and low-frequency SST anomalies, the role of subsurface gyre-scale dynamics remains unexplored. Using a set of reanalysis data sets from 1958 to the present, we find that subsurface temperature anomalies generated along the North Pacific Current significantly contribute through mean upwelling to decadal changes of SST in the Gulf of Alaska. This influence is comparable to the contribution associated with variations in atmospheric winds. Given the exceptional low-frequency character of the propagation of subsurface anomalies (e.g., multidecadal) along the gyre, monitoring subsurface temperature anomalies up stream along the North Pacific Current may enhance the decadal predictability of SST in the Gulf of Alaska and its impact on local marine ecosystems.

1. Introduction

Weather patterns and oceanic ecosystems of the North Pacific Ocean are significantly influenced by decadal climate variations. A more thorough understanding of the sources of such low-frequency climate variability is key to improving decadal prediction capabilities [*Barnett et al.*, 1999; *Liu*, 2012; *Liu et al.*, 2002; *Schneider et al.*, 2002]. Despite the many promising steps toward decadal prediction, several issues need further exploration such as clarifying the role of the ocean-atmosphere coupling and identifying the processes determining the decadal time scale of climate anomalies [*Latif and Keenlyside*, 2011; *Liu*, 2012]. At low-frequency time scales, previous studies in the North Pacific suggest that subsurface ocean dynamics play an important role in the spreading of low-oxygen waters from the western to the eastern subarctic Pacific [*Whitney et al.*, 2007]. Given the low-frequency time scales of subsurface dynamics, the purpose of this work is to understand the role of subsurface temperature anomalies in the generation of decadal sea surface temperature (SST) variability in the Northeast Pacific. Specifically, we focus on the Gulf of Alaska (GOA), one of the most productive ecosystems in the North Pacific Ocean. Here the upwelling of subsurface anomalies will be shown to contribute significantly to the GOA decadal fluctuations, which are linked to important changes in marine ecosystems.

Decadal changes in the SST of the Gulf of Alaska are linked to the Pacific Decadal Oscillation (PDO), the leading mode of SST variability in the North Pacific [*Mantua et al.*, 1997; *Schneider and Cornuelle*, 2005]. The PDO is forced predominantly by the surface expression of the Pacific North American pattern [*Wallace and Gutzler*, 1981], which is reflected in the position and the strength of Aleutian Low sea level pressure over the GOA.

Using a simple stochastic climate model, proposed by *Hasselmann* [1976]; *Cummins and Lagerloef* [2002] demonstrated that a large fraction of the SST low-frequency variability in the GOA can be reconstructed by Ekman pumping dynamics. Their model equation follows:

$$\frac{\mathrm{dSST}a}{\mathrm{d}t} = w'\overline{T}_{\mathrm{sub}} - \frac{\mathrm{SST}a}{\tau} \quad , \tag{1}$$

where changes in SST anomalies (SST*a*) over the depth of the Ekman layer are driven by anomalous upwelling (w') acting on the mean temperature at the bottom of the layer ($\overline{T}_{\mathrm{sub}}$). The second term on the right-hand side of equation (1) is associated with the damping of SST*a* over the time scale (τ). When applying this local Markov model (equation (1)), *Cummins and Lagerloef* [2002] estimated changes in Ekman velocity using a reanalysis of winds over the GOA. The damping time scale can be estimated by computing the average temporal decorrelation time scale of observed SST*a* in the GOA (~4–6 months) [e.g., *Chhak et al.*, 2009].

Although the Ekman process model (equation (1)) exhibits a strong capability of reconstructing the GOA SST*a*, this model does not consider SST*a* contributions associated with the mean upwelling of subsurface temperature anomalies generated by gyre-scale circulation dynamics. This study expands the Ekman process model of *Cummins and Lagerloef* [2002] to include the contributions of the mean upwelling ($\overline{w}$) acting on subsurface temperature anomalies at the base of the Ekman layer (T'_{sub}) as follows:

$$\frac{\mathrm{dSST}a}{\mathrm{d}t} = w'\overline{T}_{\mathrm{sub}} + \overline{w}T'_{\mathrm{sub}} - \frac{\mathrm{SST}a}{\tau}\,. \tag{2}$$

In particular, we seek to understand how changes in subsurface circulation and water properties impact the Gulf of Alaska and quantify their contribution to surface low-frequency variability.

The remainder of this paper is structured as follows. Section 2 presents the data and the isopycnal analyses. Section 3 describes the results of the propagation of subsurface temperature anomalies along the North Pacific Gyre in the Gulf of Alaska region and validates this propagation pattern with an observational data set. Section 4 investigates the role of subsurface anomalies in the sea surface temperature of the GOA, and section 5 summarizes and concludes this work.

2. Data and Methods

We investigate the subsurface temperature anomaly using two observational reanalysis data sets. The first is the European Centre for Medium-Range Weather Forecasting (ECMWF) Ocean Reanalysis System (ORA-S3). This data set has a horizontal resolution of $1° \times 1°$ in longitudinal and latitudinal directions, respectively, and 29 vertical levels spanning the period from January 1959 to December 2009 [*Balmaseda et al*., 2008]. The second reanalysis data set is the Simple Ocean Data Assimilation (SODA 2.1.6). The spatial horizontal resolution of the SODA output is $0.5° \times 0.5°$ with 40 vertical levels covering the period from January 1958 to December 2008 [*Carton and Giese*, 2008].

To explore the role of the gyre-scale circulation in generating subsurface anomalies in the GOA, we perform an isopycnal (constant-density surface) analysis. To calculate the density field, we use the SODA and ORA-S3 monthly temperature and salinity fields and follow the United Nations Educational, Scientific and Cultural Organization International Equation of State [*United Nations Educational, Scientific and Cultural Organization*, 1983]. The monthly density of each vertical level is linearly interpolated onto isopycnal surfaces using the transformation from the *z* coordinate to sigma coordinate systems, a method described in *Chu et al*. [2002]. We use the temperature anomalies on isopycnal $\sigma_\theta = 26.5$ kg m^{-3} as a proxy for subsurface temperatures that feed the GOA upwelling. This isopycnal layer does not outcrop during the winter months in either reanalysis product in the Northeast Pacific, allowing us to track changes in the properties of water masses associated with gyre-scale circulation. The 26.5 isopycnal layer is ventilated in the western subarctic Pacific, where the imprint of surface properties is transferred from the mixed layer to the ocean interior, and exchanges gases with the atmosphere. Surface processes affect this isopycnal through vertical mixing upstream of the North Pacific Gyre in the Kuroshio-Oyashio Extension (KOE) region.

To track subsurface low-frequency variance, we use temperature anomalies on isopycnal $\sigma_\theta = 26.5$ kg m^{-3}. Since temperature and salinity anomalies are compensated on a given isopycnal surface (warm/salty or cool/fresh water masses) [*Veronis*, 1972], temperature anomalies can be considered either isopycnal spiciness or salinity anomalies. We calculate the temperature anomalies of isopycnal layers by removing the monthly average and the trend from the temperature field. In addition, we compute the global average stream function based on Bernoulli's law, assuming that the density of the layer is constant along the streamline and then integrating the pressure of a column of water above each point on the isopycnal layer.

Although long-term observations of subsurface variability are rare, we use an observational data set of temperature observations on isopycnal layer $\sigma_\theta = 26.5$ kg m^{-3} from Ocean Station PAPA (P26 or OSP), located at 145°W and 50°N from August 1956 to February 2006 [*Whitney et al*., 2007]. The spatial and temporal resolutions of the OSP archive allow a description of not only the mean state but also the variability in the main state of the ocean in the Gulf of Alaska [*Freeland*, 2007]. A detailed description of the history of OSP salinity sampling is presented in *Crawford et al*. [2007].

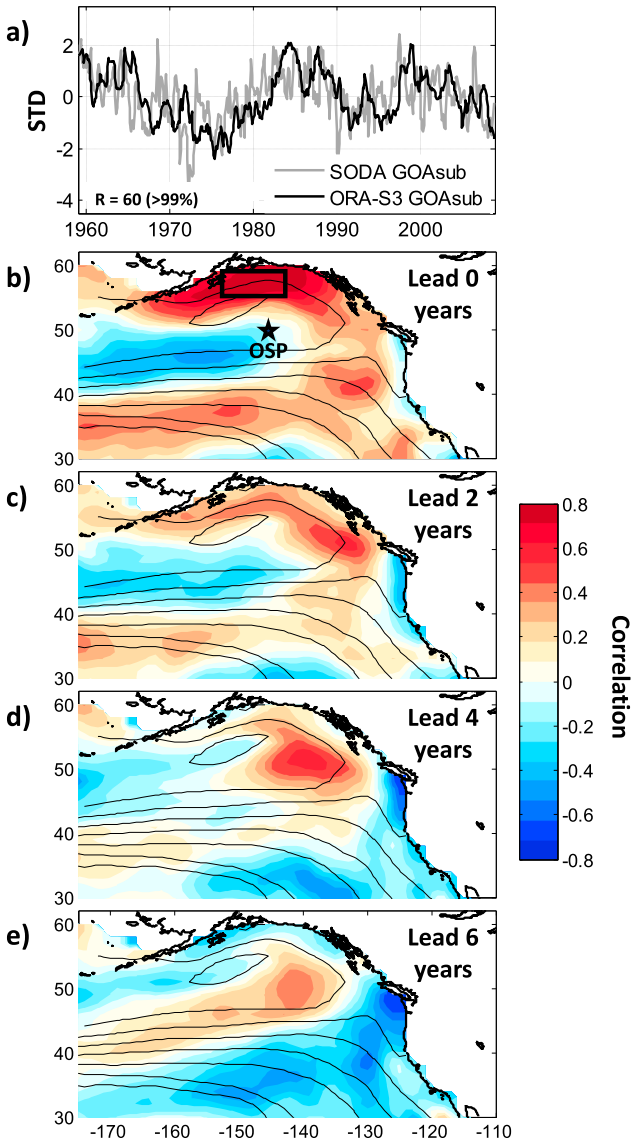

Figure 1. (a) Time series of the SODA (gray, dashed line) and ORA-S3 (black, solid line) GOAsub indexes from 1958 to 2010. Lead correlation maps between the salinity field on the $\sigma_\theta = 26.5$ kg m^{-3} isopycnal and the ORA-S3 GOAsub index at (b) lead 0 year, (c) lead 2 years, (d) lead 4 years, and (e) lead 6 years, increments of 2 years. The GOAsub index is the average salinity anomaly in the region of the black box. Contours represent the mean Bernoulli's stream function along isopycnal 26.5 from 1959 to 2010 showing the path of the gyre circulation. The black star represents the position of station PAPA or OSP (50°N, 145°W).

The sources of the SST and sea level pressure anomalies (SLP) data are the National Oceanic and Atmospheric Administration (NOAA) Extended Reconstructed SST analysis [*Smith and Reynolds*, 2003, 2004; *Smith et al*., 2008] and the National Centers for Environmental Prediction-National Center for Atmospheric Research project [*Kalnay et al*., 1996], respectively.

We estimate the significance of the correlation coefficient using a Monte Carlo technique. In this approach, each time series is approximated as an autoregressive order 1 model (AR-1) with the same lag 1 correlation coefficient computed from the original time series. We use the AR-1 models to generate 5000 realizations of two random red-noise time series and then compute the probability distribution function (PDF) of their cross-correlation coefficients. The final significance level is inferred from the correlation value associated with the 95% area under the PDF. Throughout this text, we will denote correlation coefficients by *R*.

3. Subsurface Propagation of Anomalies Along the Gyre in the GOA

To characterize subsurface circulation and anomalies in the GOA, we defined a subsurface index for the Gulf of Alaska region, the Gulf of Alaska subsurface index (GOAsub index). This index consists of spatially averaged subsurface temperature anomalies in the isopycnal 26.5 layer in the region defined by coordinates 152.5°W–142.75°W and 55.30°N–59.00°N (Figure 1b, black square). Figure 1a shows the evolution in time of the SODA (dashed gray line) and ORA-S3 (solid black line) GOAsub indexes. Although the indexes show differences in year-to-year variability, (e.g., 1965, 1968, 1990, and 2000), both time series have the same tendency and a low-frequency component. The low-frequency time scale of the GOAsub indexes is determined by double-integration effects associated with the geostrophic advection of anomalies in the subsurface by the gyre circulation dynamic [*Kilpatrick et al*., 2011; *Di Lorenzo and Ohman*, 2013]. The ORA-S3 GOAsub index is smoother, while the SODA GOAsub index is noisier. Because of the high resolution of the SODA database, the noise in the results occurs mostly in the high frequency. Therefore, both indexes are correlated by a factor of 0.6 at a >99% confidence level. The spatial correlation map between the index and the ORA-S3 subsurface temperature anomalies on the isopycnal 26.5 is above 0.8 in the region of the GOA (Figure 1b). The SODA correlation maps (not shown) are very similar to the ORA-S3 but exhibit

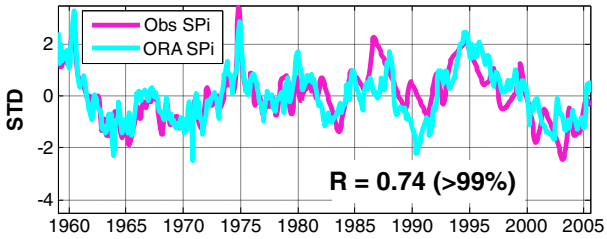

Figure 2. (a) Time series of the salinity anomalies from Station PAPA (Obs *SP* index) (purple line) and from the ORA-S3 data set (ORA *SP* index) (light blue line) from 1959 to 2005 (correlation $R = 0.74$, >99% confidence).

more noise in space. Given our interest in understanding the large-scale and low-frequency components of the subsurface temperature signal, we have selected the coarser resolution ORA-S3 maps to present the subsurface analyses.

The temporal evolution of the GOAsub signal in the subsurface is characterized using lead/lag correlation maps between the GOAsub index at year 0 and the isopycnal temperature anomalies during previous years (e.g., lead 0, 2, 4, and 6 years) in Figures 1b–1e. The figure shows that during previous lead times, a signal of this correlation propagates with the mean circulation. At lead 0 year, the maximum correlation between the GOAsub index and the subsurface temperature anomalies on the isopycnal 26.5 ($R = 0.8$) is in the northern GOA in the region where the index was defined (Figure 1b). At lead 2 years (Figure 1c), the peak correlation has shifted upstream of the Alaskan Gyre along the coast of British Columbia. At lead 4 years, the peak correlation has shifted farther to the south of the northern GOA. At lead 6 years, the southwest backward propagation of the GOAsub signal along the mean gyre circulation becomes even more evident. By lead years 4 and 6, the signal, now weaker ($R = 0.4$–0.6), has moved away from the northern GOA and stretches along the axis of the North Pacific Current. At lead 8 years, the signal weakens ($R = 0.2$) (not shown) and is centered at 150°W and 45°N. The same analysis conducted for future lag times shows the northern GOA subsurface signal stretching and disappearing along the Aleutians (not shown), consistent with the Alaskan Gyre circulation.

The same analysis is performed with the SODA data set (not shown), which reveals similar propagation patterns. A weak signal in the southwest GOA region that propagates following circulation reaches the GOA region at lag 0 and stretches at later lag times. The main difference is that the signal is noisier in SODA.

To check the consistency of the reanalysis products in capturing subsurface signals, we compare a time series of subsurface temperature anomalies from the ORA-S3 data set with in situ subsurface observations at Station PAPA (OSP). The temperature anomalies in the OSP are used to build an index, Station PAPA, or the *SP* index. Figure 2 shows the time series of the observed (purple line) and ORA-S3 (light blue line) *SP* indexes, both of which are correlated by a correlation factor of 0.74 (>99% of confidence). Until 1980, both indexes evolved almost simultaneously, with two large anomalous values recorded in 1961 and 1975. Between 1980 and 1995, the *SP* index exhibits differences between the two data sets, and afterward, the anomalies exhibit the same trend in both indexes. The propagation of temperature anomalies along the mean gyre circulation, shown in the correlation map analysis between the ORA-S3 GOAsub index and the temperature anomalies on the $\sigma_\theta = 26.5$ kg m^{-3} isopycnal (Figure 1), were found to be consistent with the propagation of anomalies inferred from lead/lag correlation maps between the ORA-S3 *SP* index and the temperature anomalies on the same isopycnal layer (not shown in figures).

4. The Role of GOA Subsurface Anomalies in Surface Temperature

To explore the role of subsurface anomalies in modulating low-frequency SSTa in the GOA, we expand the Ekman pumping model of *Cummins and Lagerloef* [2002] by suggesting that variability in upper ocean temperature anomalies in the GOA is driven by changes in both upwelling velocity, resulting from wind anomalies, and the subsurface water mass properties. We therefore propose the model described in equation (2) for the low-frequency SST*a* in the GOA.

We test the expanded Ekman process model (equation (2)) in a control volume over the GOA (red box in Figure 3a), where we define the index of SST anomalies (GOA-SST*a* index) (red line in Figure 3b) as the average of monthly SST anomalies extracted from the NOAA from 1950 to 2011. Figure 3a shows the correlation map of this index and SST anomalies in the Gulf of Alaska. This correlation pattern reproduces the spatial signature of the PDO: the negative values of SST anomalies in the Central North Pacific and positive values along the West Coast and in the Gulf of Alaska [*Mantua et al.*, 1997]. This pattern is also evident by the significant correlation between the time series of the GOA-SST*a* and PDO indexes (Figure 3b).

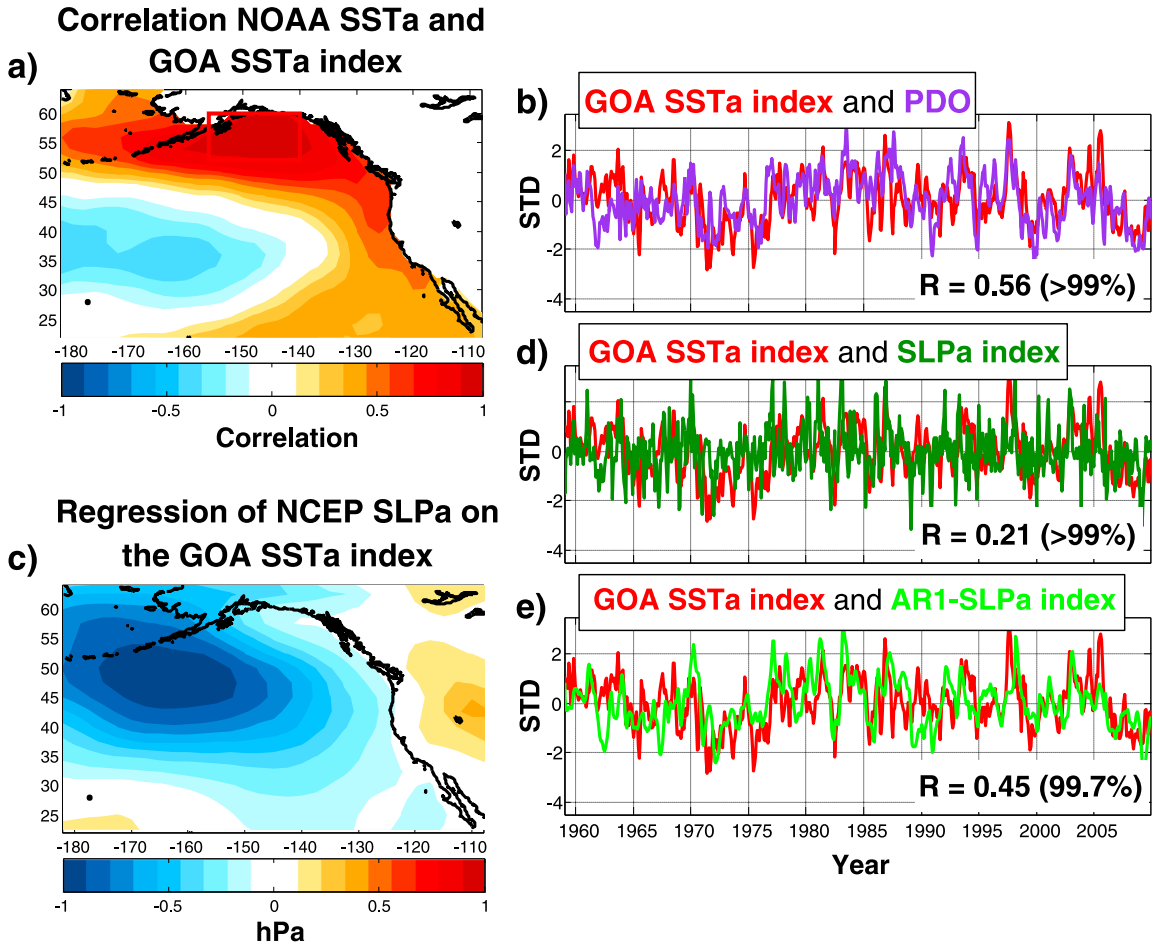

Figure 3. (a) Correlation map between SST anomalies and the GOA-SST*a* index. The latter is the average temperature anomaly in the region of the red box. (b) Time series of the GOA-SST*a* index (red line) compared to the PDO index (purple line) from 1959 to 2009 (correlation $R = 0.56$, >99% significance). (c) Regression of SLPa on the GOA SST*a* index. (d) Time series of the GOA-SST*a* index (red line) compared to the SLP*a* index (dark green line) (correlation R = 0.21, >99% significance). (e) The GOA-SSTa index (red line) compared to the SLPa index (light green line) from the AR1-model (correlation $R = 0.45$, 99.7% significance).

To recover the *Cummins and Lagerloef* [2002] model, we define an index of wind-induced Ekman pumping (w') using sea level pressure anomalies (SLP*a*) over the GOA. The goal is to define a w' index that is optimal in capturing SST*a* variability so that we can quantify how much of the SST*a* variability can be explained by surface atmospheric forcing versus how much is driven by subsurface processes. First, we compute a regression map of the SLP*a* on the GOA-SST*a* index (Figure 3c) to isolate the optimal spatial pattern of atmospheric forcing. Consistent with previous findings [*Chhak et al.*, 2009], the atmospheric forcing pattern of GOA-SST*a* shows the predominant signature of the Aleutian low, characterized by basin-scale negative SLP anomalies between 20°N and 60°N. This characteristic SLP anomaly pattern in the GOA defines the best pattern of the atmospheric forcing of SST anomalies. We now use this pattern to build an index for the atmospheric forcing of the SST by projecting the SLP*a* field onto the pattern. This projection operation yields the SLP*a* index. This approach ensures that the SLP*a* index captures most of the atmospheric induced variability of SST*a*. A correlation between the raw monthly SLP*a* index and the GOA-SST*a* index exhibits a significant correlation of 0.21 (*a* >99% significance level) (Figure 3d, dark green and red lines, respectively).

Neglecting the subsurface mean upwelling term ($\overline{w}$ in equation (2)) acting on the subsurface anomalies (T'_{sub}), we recover the model of *Cummins and Lagerloef* [2002] (equation (1)), which is equivalent to an autoregressive model of order 1 (AR-1). To reconstruct GOA-SST*a* index variability driven by atmospheric forcing, we take the SLP*a* index as a proxy of atmospheric forcing, using it as the forcing function in the AR-1 model. Because SLP*a* are correlated with changes in heat fluxes over the GOA, the SLP*a* forcing function contains the effects of both direct Ekman pumping and surface heating over the SST*a*. Given that the effects

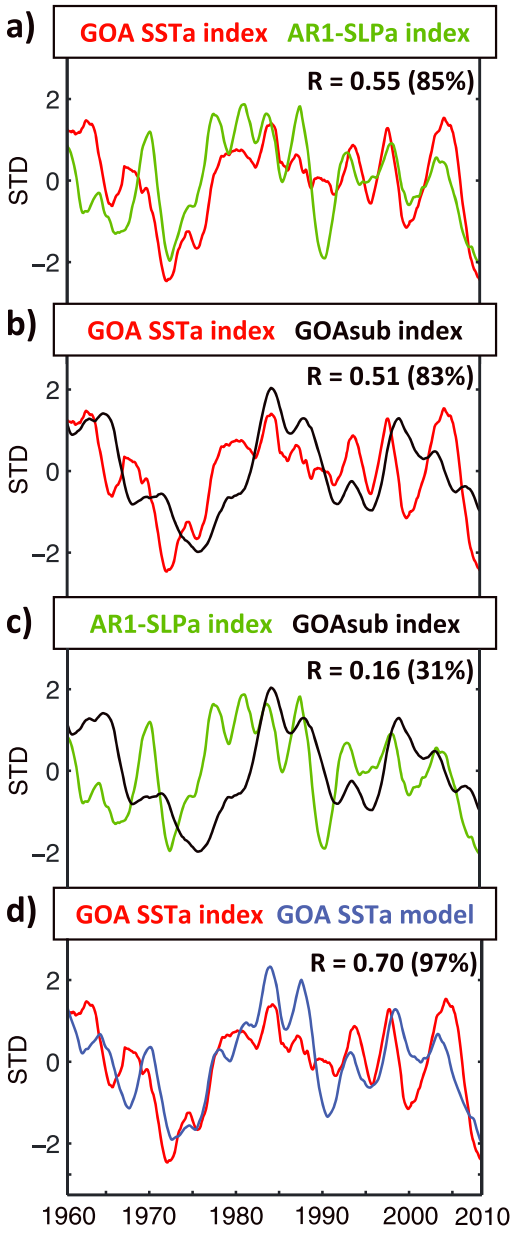

Figure 4. Six-year low-pass filtered times series of (a) the GOA-SST*a* index (red line) compared to the AR1-SLP*a* index (green line) (correlation $R = 0.55$, 85.2% significance); (b) the GOAsub index (black line) compared to the GOA-SST*a* index (red line) (correlation $R = 0.51$, 83% significance); (c) the GOAsub index (black line) compared to the AR1-SLP*a* index (green line) (correlation $R = 0.16$, 31.1% significance); and (d) the GOA-SST*a* index (red line) compared to the GOA-SST*a* index modeled by equation (2) (blue line) (correlation $R = 0.70$, 97.4% significance).

of both Ekman pumping and surface heating can be represented as an AR-1 model, we refer to the AR-1 model hindcast as the fraction of variability in SST*a* driven by atmospheric forcing. In the AR-1 model, SST*a* damping scale τ, computed from the autocorrelation time scale of the GOA-SST*a* index, is set to 6 months. This value of the damping scale is consistent with that of previous studies [e.g., *Chhak et al.*, 2009]. By selecting a longer time scale for damping (e.g., 12–18 months), as in *Cummins and Lagerloef* [2002], we obtain similar results with a smoother SST*a* time series. To solve the AR-1 model, we use a simple Euler forward time step scheme. The AR-1 model forced by the SLP anomalies (AR1-SLP index, the light green line in Figure 3e) filters the high-frequency component associated with atmospheric forcing and produces a signal characterized by stronger low frequency [*Rudnick and Davis*, 2003]. Using this reconstruction, we observe that the variance of the SST explained by atmospheric forcing increases significantly (R = 0.45, a 99.7% significance level). To estimate the contribution of the surface forcing to the low-frequency variance of the SST*a*, we apply a 6 year low-pass filter to the AR1-SLP*a* index (Figure 4a). The correlation between the 6 year filtered GOA-SST*a* and the AR1-SLP*a* index has a low statistical significance ($R = 0.55$, an 85.2% significance level, Figure 4a), suggesting that other processes in addition to Ekman pumping and surface heating (atmospheric forcing) contribute to the decadal variance of the SST in the GOA.

We now explore the contributions of the mean upwelling of subsurface anomalies to SST*a* variability using equation (2). We use the GOAsub index (Figure 1) as a proxy for variability driven by the subsurface anomalies ($\overline{w}T'_{sub}$). Given that the GOAsub index is already dominated by low-frequency variability, the integration of equation (2) does not change the character of the GOAsub index. Therefore, to quantify the contributions of GOAsub to the decadal variations of the SST*a*, we simply apply a 6 year low-pass filter to the GOAsub (Figure 4b). The results suggest that subsurface anomalies flowing upward by the mean upwelling explain an equal fraction of the decadal variability of the SST ($R = 0.51$) when compared to that of the surface Ekman pumping in the Gulf of Alaska region ($R = 0.55$) (compare Figures 4a and 4b). To examine the degree to which these surface and subsurface forcings of the SST*a* are independent, Figure 4c shows the low-pass GOAsub and AR1-SLP*a* index time series and their correlation coefficient. The low correlation ($R = 0.16$, a 31% significance level) between these two indexes shows that atmospheric forcing (anomalous upwelling velocity) and subsurface forcing (temperature anomalies on the isopycnal 26.5) are largely independent, indicating that each forcing captures a different aspect of the low-frequency variance of the SST.

Since atmospheric and subsurface forcings are independent, they can be combined in a linear model for the SST*a* in the Gulf of Alaska,

$$\mathrm{SST}a(t) = \alpha(\mathrm{AF}) + \beta(\mathrm{SF}), \quad (3)$$

where AF is atmospheric forcing (anomalous upwelling velocity), represented as the AR1-SLP*a* index, and SF is subsurface forcing (subsurface temperature anomalies on the isopycnal 26.5 advected by the mean upwelling), represented as the GOAsub index. Parameters $\alpha = 0.39$ and $\beta = 0.29$ are obtained using least squares. Figure 4d shows the results of the low-pass filter linear model (equation (3)) for the GOA-SST*a* (Figure 4d, blue line) and GOA-SST*a* indexes (Figure 4d, red line). The low-pass filter is shown to highlight the decadal variance of the indexes. The correlation factor without a filter applied (not shown) is $R = 0.53$ ($a > 99\%$ significance level) and with a 6 year filter applied is $R = 0.70$ (a 97.4% significance level). These results indicate that the linear model proposed here and forced by Ekman pumping and subsurface temperature anomalies explains almost half of the low-frequency variance of the SST in the GOA.

5. Discussion and Conclusion

This study examined the role of subsurface temperature anomalies on the isopycnal layer $\sigma_\theta = 26.5$ kg m^{-3} in modulating the low-frequency variability of the SST in the GOA. The results reveal that temperature anomalies advected in the subsurface by the gyre-scale circulation exhibit significant low-frequency variability and contribute through mean upwelling to an important fraction of decadal variance of SST in the GOA upwelling system. Advected by the mean circulation, these subsurface anomalies are tracked back into the North Pacific Current. The dynamics generating the subsurface anomalies remain unclear.

Previous studies suggest that these subsurface anomalies along the axis of the North Pacific Current could be initiated by surface buoyancy forcing [*Nonaka and Xie*, 2000] and by anomalous advection upstream of the subtropical subduction regions in the Kuroshio-Oyashio Extension (KOE) region [*Taguchi and Schneider*, 2014]. Once these subsurface anomalies are generated in their source regions, they are advected by the main geostrophic current toward the eastern Pacific. Using a conservative water-mass tracer along isopycnals, *Whitney et al*. [2007] reported a propagation of oxygen anomalies from the KOE region eastward across the Pacific. The present study shows how temperature anomalies reach also the subarctic gyre and the GOA, where they mixed into the upper ocean through upwelling. However, it remains unclear if and how much the subsurface anomalies are attenuated during the course of their propagation from the KOE to GOA regions or if other processes contribute to generation of subsurface anomalies along the axis of the gyre in the central and eastern North Pacific.

While future studies should identify the dynamics underlying the initiation and attenuation of these anomalies along their propagation path, this study suggests that tracking the propagation of subsurface anomalies may enhance our ability to make decadal predictions of surface variability in the Gulf of Alaska and the PDO pattern. By identifying the role of the advected subsurface anomalies generated along the North Pacific Current, this work contribute to our understanding of the mechanisms/sources of decadal variability in the Gulf of Alaska and its impact on local marine ecosystems. Given the exceptional low-frequency character of the propagation of subsurface anomalies along the gyre, future study should conduct long-term, high-resolution ocean model simulations to further diagnose the processes generating the anomalies and how robust are the decadal predictions.

Acknowledgments

The authors are thankful to Taka Ito for providing the processed temperature observations of the isopycnal layer from Ocean Station PAPA. The original time series of temperature observations from Ocean Station PAPA comes from Fisheries and Oceans Canada at http://www.pac.dfo-mpo.gc.ca/science/oceans/data-donnees/line-p/data-eng.html. The two observational reanalysis data sets used in this study, ECMWF ORA-S3 and SODA (v2.1.6), are available from the Asia-Pacific Data-Research Center (APDRC) at the University of Hawaii (http://apdrc.soest.hawaii.edu/data/data.php). The SST and SLP data are from the Physical Sciences Division of the National Oceanic and Atmospheric Administration (NOAA) Earth System Research Laboratory at http://www.esrl.noaa.gov/psd/data/gridded/. The processed data on the isopycnal layer that the authors used to construct figures in this work and output from the AR-1 model are also available from the first author, Mercedes Pozo Buil (mercedes.pozo@eas.gatech.edu). This work was supported by the Pacific Ocean Eddies and Climate Study (www.pex.org) NSF-OCE 1356924.

The Editor thanks two anonymous reviewers for their assistance in evaluating this paper.

References

Balmaseda, M. A., A. Vidard, and D. L. T. Anderson (2008), The ECMWF Ocean Analysis System: ORA-S3, *Mon. Weather Rev.*, *136*(8), 3018–3034.

Barnett, T. P., D. W. Pierce, R. Saravanan, N. Schneider, D. Dommenget, and M. Latif (1999), Origins of the midlatitude Pacific decadal variability, *Geophys. Res. Lett.*, *26*(10), 1453–1456, doi:10.1029/1999GL900278.

Carton, J. A., and B. S. Giese (2008), A reanalysis of ocean climate using Simple Ocean Data Assimilation (SODA), *Mon. Weather Rev.*, *136*(8), 2999–3017.

Chhak, K. C., E. Di Lorenzo, N. Schneider, and P. F. Cummins (2009), Forcing of low-frequency ocean variability in the Northeast Pacific*, *J. Clim.*, *22*(5), 1255–1276.

Chu, P. C., R. F. Li, and X. B. You (2002), Northwest Pacific subtropical countercurrent on isopycnal surface in summer, *Geophys. Res. Lett.*, *29*(17), 1842, doi:10.1029/2002GL014831.

Crawford, W., J. Galbraith, and N. Bolingbroke (2007), Line P ocean temperature and salinity, 1956–2005, *Prog. Oceanogr.*, *75*(2), 161–178.

Cummins, P. F., and G. S. E. Lagerloef (2002), Low-frequency pycnocline depth variability at Ocean Weather Station P in the Northeast Pacific, *J. Phys. Oceanogr.*, *32*(11), 3207–3215.

Di Lorenzo, E., and M. D. Ohman (2013), A double-integration hypothesis to explain ocean ecosystem response to climate forcing, *Proc. Natl. Acad. Sci. U.S.A.*, *110*(7), 2496–2499.
Freeland, H. (2007), A short history of ocean station papa and Line P, *Prog. Oceanogr.*, *75*(2), 120–125.
Hasselmann, K. (1976), Stochastic climate models.1. Theory, *Tellus*, *28*(6), 473–485.
Kalnay, E., et al. (1996), The NCEP/NCAR 40-year reanalysis project, *Bull. Am. Meteorol. Soc.*, *77*(3), 437–471.
Kilpatrick, T., N. Schneider, and E. Di Lorenzo (2011), Generation of low-frequency spiciness variability in the thermocline, *J. Phys. Oceanogr.*, *41*(2), 365–377.
Latif, M., and N. S. Keenlyside (2011), A perspective on decadal climate variability and predictability, *Deep Sea Res. Part II*, *58*(17–18), 1880–1894.
Liu, Z. (2012), Dynamics of interdecadal climate variability: A historical perspective*, *J. Clim.*, *25*(6), 1963–1995.
Liu, Z., L. Wu, R. Gallimore, and R. Jacob (2002), Search for the origins of Pacific decadal climate variability, *Geophys. Res. Lett.*, *29*(10), 1404, doi:10.1029/2001GL013735.
Mantua, N. J., S. R. Hare, Y. Zhang, J. M. Wallace, and R. C. Francis (1997), A Pacific interdecadal climate oscillation with impacts on salmon production, *Bull. Am. Meteorol. Soc.*, *78*(6), 1069–1079.
Nonaka, M., and S.-P. Xie (2000), Propagation of North Pacific interdecadal subsurface temperature anomalies in an ocean GCM, *Geophys. Res. Lett.*, *27*(22), 3747–3750, doi:10.1029/2000GL011488.
Rudnick, D. L., and R. E. Davis (2003), Red noise and regime shifts, *Deep Sea Res. Part I*, *50*(6), 691–699.
Schneider, N., and B. D. Cornuelle (2005), The forcing of the Pacific decadal oscillation, *J. Clim.*, *18*(21), 4355–4373.
Schneider, N., A. J. Miller, and D. W. Pierce (2002), Anatomy of North Pacific decadal variability, *J. Clim.*, *15*(6), 586–605.
Smith, T. M., and R. W. Reynolds (2003), Extended reconstruction of global sea surface temperatures based on COADS data (1854–1997), *J. Clim.*, *16*(10), 1495–1510.
Smith, T. M., and R. W. Reynolds (2004), Improved extended reconstruction of SST (1854–1997), *J. Clim.*, *17*(12), 2466–2477.
Smith, T. M., R. W. Reynolds, T. C. Peterson, and J. Lawrimore (2008), Improvements to NOAA's historical merged land-ocean surface temperature analysis (1880–2006), *J. Clim.*, *21*(10), 2283–2296.
Taguchi, B., and N. Schneider (2014), Origin of decadal-scale, eastward-propagating heat content anomalies in the North Pacific, *J. Clim.*, *27*(20), 7568–7586.
United Nations Educational, Scientific and Cultural Organization (1983), Algorithms for computation of fundamental properties of seawater, 1983, *Unesco Tech. Pap. in Mar. Sci.*, *44*, 53 pp.
Veronis, G. (1972), Properties of seawater defined by temperature, salinity, and pressure, *J. Mar. Res.*, *30*(2), 227–255.
Wallace, J. M., and D. S. Gutzler (1981), Teleconnections in the geopotential height field during the Northern Hemisphere winter, *Mon. Weather Rev.*, *109*(4), 784–812.
Whitney, F. A., H. J. Freeland, and M. Robert (2007), Persistently declining oxygen levels in the interior waters of the eastern subarctic Pacific, *Prog. Oceanogr.*, *75*(2), 179–199.